Inorg. Chem. **2002**, *41*, 4915–4922

Organometallic Pt(II) Compounds. A Complementary Study of a Triplet Emitter Based on Optical High-Resolution and Optically Detected Magnetic Resonance Spectroscopy

Hartmut Yersin,* Dirk Donges, Werner Humbs, and Johann Strasser

Institut für Physikalische und Theoretische Chemie, Universität Regensburg, D-93040 Regensburg, Germany

Rolf Sitters and Max Glasbeek*

Laboratory for Physical Chemistry, University of Amsterdam, Nieuwe Achtergracht 129, 1018 WS Amsterdam, The Netherlands

Received February 15, 2002

The emitting triplet state of cyclometalated Pt(thpy)(CO)(Cl) monomers ((thpy)$^-$ = 2-(2′-thienylpyridinate), frequently also abbreviated as (2-thpy)$^-$) is investigated at T = 1.2 K (typically) by use of the *complementary* methods of high-resolution optical spectroscopy and of optically detected magnetic resonance (ODMR) spectroscopy. Such a complimentary investigation is carried out for the first time for a Pt(II) compound. In solution, oligomer or short linear chain formation is also observed. However, the monomers can be investigated selectively, when they are dissolved in a relatively inert *n*-octane matrix (Shpol'skii matrix). This allows us to determine the energies of the T_1 triplet substates I, II, and III relative to the electronic ground state $S_0(0)$, the zero-field splittings (ZFSs) of T_1, and emission decay time constants (I/II ↔ 0, 18012.5 cm^{-1}; III ↔ 0, 18016.3 cm^{-1}; $\Delta E_{I,II}$ = 0.05437 cm^{-1} (1.631 GHz), $\Delta E_{I,III}$ = 3.8 cm^{-1} (114 GHz); τ_I = 120 μs, τ_{II} = 45 μs, τ_{III} = 35 μs; spin–lattice relaxation time for the processes III ⇝ I/II, τ_{SLR} = 3.0 μs). The vibrational satellite structure observed in the emission of the T_1 state to the singlet ground state S_0 is also discussed. Moreover, it is possible to estimate the intersystem crossing time from the excited singlet state S_1 at 22952 cm^{-1} to the triplet state T_1 to ∼5 ps. The T_1 state is assigned as a thpy-ligand-centered $^3\pi\pi^*$ state with small metal-to-ligand charge-transfer (MLCT) admixtures. A comparison of Pt(thpy)(CO)(Cl) to a series of other organometallic Pt(II) compounds, such as heteroleptic Pt(ppy)(CO)(Cl) ((ppy)$^-$ = phenylpyridinate), Pt(dppy)(CO) ((dppy)$^{2-}$ = diphenylpyridinate), and Pt(i-biq)(CN)$_2$ (i-biq = 2,2′-bisisoquinoline) and homoleptic Pt(thpy)$_2$ and Pt(ppy)$_2$, is carried out. (The structures are shown in Figure 7.) Trends of photophysical properties are discussed. In particular, by chelation of two equal ligands the pattern of ZFS is strongly altered, resulting in a significant increase of the MLCT participation in the lowest triplet state of these organometallic compounds. This new observation represents an interesting further step concerning chemical tunability of photophysical properties.

1. Introduction

Pt(II) compounds with organic ligands have attracted much attention since they may potentially be used for very different kinds of new materials, ranging from antitumor compounds[1–3] to new electroluminescent devices, such as *organometallic* light-emitting devices with triplet harvesting properties.[4,5] In this latter field promising developments are expected as

* Authors to whom correspondence should be addressed. E-mail: hartmut.yersin@chemie.uni-regensburg.de (H.Y.); glasbeek@science.uva.nl (M.G.). Homepage: http://www.uni-regensburg.de/∼hartmut.yersin (H.Y.).

(1) Rosenberg, B.; Van Camp, L.; Krigas, T. *Nature (London)* **1965**, *205*, 698.
(2) Gelasco, A.; Lippard, S. J. *Top. Biol. Inorg. Chem.* **1999**, *1*, 1.
(3) Kritzenberger, J.; Berhardt, G.; Gust, R.; Pistor, P.; Schönenberger, H.; Yersin, H. *Monatsh. Chem.* **1993**, *124*, 587.
(4) Guo, T.-F.; Chang, S.-C.; Yang, Y.; Kwong, R. C.; Thompson, M. E. *Org. Electron.* **2000**, *1*, 15.
(5) Baldo, M. A.; Lamansky, S.; Burrows, P. E.; Thompson, M. E.; Forrest, S. R. *Appl. Phys. Lett.* **1999**, *75*, 4.

10.1021/ic020132o CCC: $22.00
Published on Web 08/29/2002

compared to the already established *organic* light-emitting devices (OLEDs).[6−8] In particular, the lowest triplet states of Pt(II) complexes frequently exhibit a bright phosphorescence to the singlet ground states. Moreover, one finds a pronounced diversity with respect to emission wavelengths, decay times, and quantum yields.[9−18] An enormous variability is also found regarding sizes and patterns of zero-field splittings (ZFSs) of the triplets into the three substates,[18,19] excitation dynamics within the triplet substate system according to different spin−lattice relaxation (SLR) processes,[19−21] vibronic coupling properties,[18] spatial extensions of excited-state wave functions,[18,22] etc. These features may systematically be tuned by the variation of the ligands coordinating the Pt(II) central metal ion. By this procedure, one can adjust the participation of metal Pt 5d or metal-to-ligand charge-transfer (MLCT) character relative to the ligand $\pi\pi^*$ character of the triplet state.[18] Accordingly, the effective spin−orbit coupling is also strongly varied. For most compounds investigated so far, spin−orbit coupling is relatively large. This results in ZFSs of many wavenumbers. Thus, the corresponding values are about 2 orders of magnitude larger than usually found for pure organic molecules.

Detailed characterizations of triplet states of organometallic Pt(II) compounds with significant metal participation and consequently relatively large ZFSs have recently been carried out.[18−24] On the other hand, it is attractive, and in fact, it is the objective of this investigation to study a compound with a small metal perturbation (small ZFS) of a triplet state. This situation is not frequently found for Pt(II) compounds. However, the cyclometalated Pt(thpy)(CO)(Cl) complex (see the inset of Figure 1) represents such an example, and therefore, it is expected that this compound exhibits specific emission features. Moreover, as will be shown, the characterization of the triplet state can be realized on the basis of the complementary methods of high-resolution optical spectroscopy and of ODMR (optically detected magnetic resonance) spectroscopy. Corresponding complementary investigations have already very successfully been carried out for Pd(II) compounds[18,25−28] and Rh(III) compounds,[29−34] but they are applied here for the first time to the lowest triplet state of a Pt(II) compound.

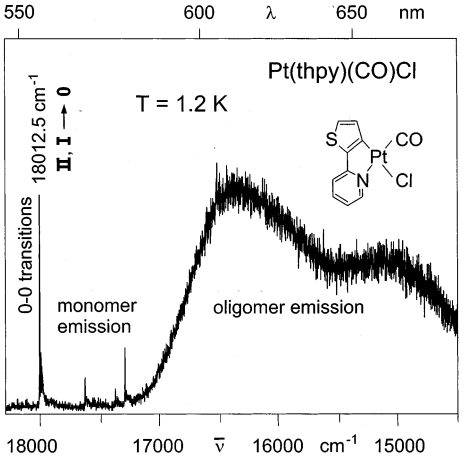

Figure 1. Emission of Pt(thpy)(CO)(Cl) in an *n*-octane Shpol'skii matrix ($c \approx 10^{-5}$ mol/L) at $T = 1.2$ K. The excitation wavelength is $\lambda_{exc} = 363.8$ nm (27488 cm^{-1}) and thus nonselective with respect to an excitation of monomers and oligomers.

2. Experimental Section

Pt(thpy)(CO)(Cl) was prepared in analogy[35] to the procedures described[36] for the preparations of various heteroleptic 2-(2′-thienyl)pyridine complexes of Pt(II). The compound is spectroscopically investigated in an *n*-alkane Shpol'skii[37] matrix at low temperature. However, since Pt(thpy)(CO)(Cl) is not directly soluble in *n*-alkanes, it was first dissolved in an intermediate solvent (1,4-dioxane). Subsequently, this solution was diluted with *n*-octane to a ratio of 1:50 v/v. The final concentration of Pt(thpy)(CO)(Cl) was about 10^{-5} mol/L. The solution was poured into a quartz cuvette (inner diameter 1 mm) and cooled with a cooling rate of about 100 K/min.[23] Thus, the Shpol'skii matrix was obtained. The optical high-resolution measurements were accomplished with experimental equipment[22] and an optical setup[38] as specified previously. The ODMR spectrometer used was the same as also described elsewhere.[25,39] Optical excitation for these ODMR experiments was at 340 mm (∼29400 cm^{-1}) using a 100 W high-pressure mercury lamp and an UG11 filter. ODMR spectra were recorded for the sample

(6) Kido, J.; Kimura, M.; Nagai, K. *Science* **1995**, *267*, 1332.
(7) Salbeck, J. *Ber. Bunsen-Ges. Phys. Chem.* **1996**, *100*, 1667.
(8) Sixl, H.; Schenk, H.; Yu, N. *Phys. Bl.* **1998**, *54*, 3.
(9) Cummings, S. D.; Eisenberg, R. *J. Am. Chem. Soc.* **1996**, *118*, 1949.
(10) Lu, W.; Chan, M. C. W.; Cheung, K.-K.; Che, C.-M. *Organometallics* **2001**, *20*, 2477.
(11) Michalec, J. F.; Bejune, S. A.; Cuttell, D. G.; Summerton, G. C.; Gertenbach, J. A.; Field, J. S.; Haines, R. J.; McMillin, R. D. *Inorg. Chem.* **2001**, *40*, 2193.
(12) Cave, G. W. V.; Fanizzi, F. P.; Deeth, R. J.; Errington, W.; Rouke, J. P. *Organometallics* **2000**, *19*, 1355.
(13) Funayama, T.; Kato, M.; Kosugi, H.; Yagi, M.; Higuchi, J.; Yamauchi, S. *Bull. Chem. Soc. Jpn.* **2000**, *73*, 1541.
(14) Mdleleni, M. M.; Bridgewater, J. S.; Watts, R. J.; Ford, P. C. *Inorg. Chem.* **1995**, *34*, 2334.
(15) Kvam, P.-I.; Puzyk, M. V.; Cotlyr, V. S.; Balashev, K. P.; Songstad, J. *Acta Chem. Scand.* **1995**, *49*, 645.
(16) Balashev, K. P.; Puzyk, M. V.; Kotlyar, V. S.; Koulikova, M. V. *Coord. Chem. Rev.* **1997**, *159*, 109.
(17) Chassot, L.; von Zelewsky, A. *Inorg. Chem.* **1987**, *26*, 2814.
(18) Yersin, H.; Donges, D. *Top. Curr. Chem.* **2001**, *214*, 81.
(19) Strasser, J.; Donges, D.; Humbs, W.; Koulikova, M. V.; Balashev, K. P.; Yersin, H. *J. Lumin.* **1998**, *76−77*, 611.
(20) Strasser, J.; Homeier, H. H. H.; Yersin, H. *Chem. Phys.* **2000**, *255*, 301.
(21) Yersin, H.; Strasser, J. *Coord. Chem. Rev.* **2000**, *208*, 331.
(22) Yersin, H.; Humbs, W. *Inorg. Chem.* **1999**, *38*, 5820.
(23) Wiedenhofer, H.; Schützenmeier, S.; von Zelewsky, A.; Yersin, H. *J. Phys. Chem.* **1995**, *99*, 13385.
(24) Yersin, H.; Strasser, J. *J. Lumin.* **1997**, *72−74*, 462.
(25) Glasbeek, M. *Top. Curr. Chem.* **2001**, *213*, 95.
(26) Glasbeek, M.; Sitters, R.; van Veldhoven, E.; von Zelewsky, A.; Humbs, W.; Yersin, H. *Inorg. Chem.* **1998**, *37*, 95.
(27) Yersin, H.; Donges, D.; Nagle, J. K.; Sitters, R.; Glasbeek, M. *Inorg. Chem.* **2000**, *39*, 770.
(28) Schmidt, J.; Wiedenhofer, H.; von Zelewsky, A.; Yersin, H. *J. Phys. Chem.* **1995**, *99*, 226.
(29) Komada, Y.; Yamauchi, S.; Hirota, N. *J. Phys. Chem.* **1986**, *90*, 6425.
(30) Van Oort, E.; Sitters, R.; Scheijde, J. H.; Glasbeek, M. *J. Chem. Phys.* **1987**, *87*, 2394.
(31) Kamyshny, A. L.; Suisalu, A. P.; Aslanov, L. A. *Coord. Chem. Rev.* **1992**, *117*, 1.
(32) Westra, J.; Glasbeek, M. *Chem. Phys. Lett.* **1991**, *180*, 41.
(33) Giesbergen, C. P. M.; Terletski, C.; Frei, G.; Zilian, A.; Güdel, H. U.; Glasbeek, M. *Chem. Phys. Lett.* **1993**, *213*, 597.
(34) Giesbergen, C. P. M.; Glasbeek, M. *J. Phys. Chem.* **1993**, *97*, 9942.
(35) Donges, D. Ph.D. Thesis, Universität Regensburg, Germany, 1997.
(36) Kvam, P.-I.; Songstad, J. *Acta Chem. Scand.* **1995**, *49*, 313.
(37) Shpol'skii, E. V. *Sov. Phys. Usp. (Engl. Transl.)* **1960**, *3*, 372.
(38) Stock, M.; Yersin, H. *Chem. Phys. Lett.* **1976**, *40*, 423.
(39) Glasbeek, M.; Hond, R. *Phys. Rev. B* **1981**, *23*, 4220.

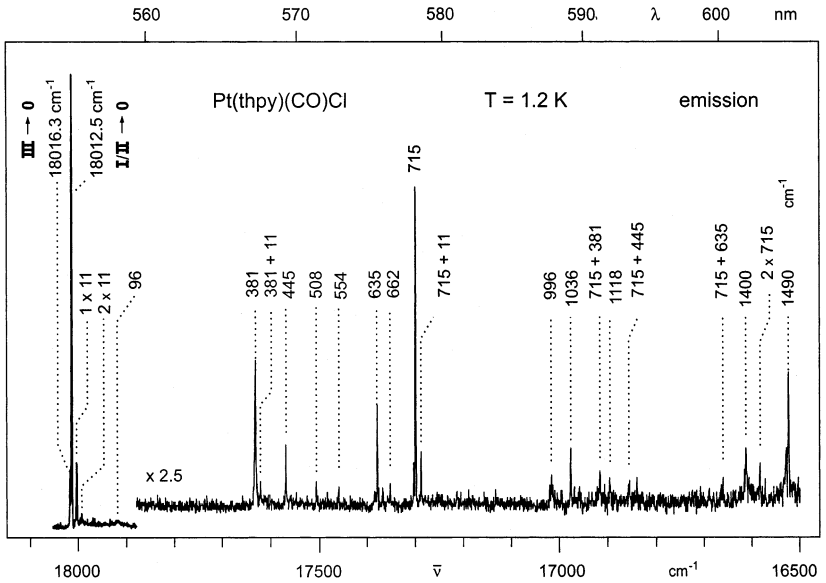

Figure 2. Triplet emission of Pt(thpy)(CO)(Cl) monomers in *n*-octane at $T = 1.2$ K. Selective excitation at 22952 cm^{-1} (435.69 nm), which corresponds to the $S_0 \rightarrow S_1$ 0−0 transition of the monomer. The vibrational energies are specified relative to the electronic 0−0 transition from the triplet substates I/II to the singlet ground state 0 (S_0) at 18012.5 cm^{-1}.

in a bath of liquid helium pumped down to 1.4 K. Small magnetic fields (up to 400 G) were applied by means of superconducting Helmholtz coils immersed in the liquid helium bath. Microwave recovery transients were optically detected by applying resonant microwave pulses of 100 μs duration at a repetition rate of 640 Hz. Optical detection was by means of a GaAs photomultiplier tube (Hamamatsu, type R 943-2). All data were collected and analyzed by on-line computer processing.

3. Results and Discussion

3.1. Dual Emission. Figure 1 shows an emission spectrum of Pt(thpy)(CO)(Cl) dissolved in *n*-octane at a concentration of about 10^{-5} mol/L and measured at $T = 1.2$ K. The excitation wavelength was $\lambda_{exc} = 363.8$ nm (27488 cm^{-1}). Apparently, the spectrum consists of two different parts, a structured emission between about 18000 and 17000 cm^{-1} and a very broad emission between about 17000 and 14000 cm^{-1}. It is proposed that the whole spectrum results from different species.

It is indicated that *the broad-band emission* in the orange-red region stems from oligomers which consist of small numbers of electronically interacting Pt(thpy)(CO)(Cl) units that are already present in the frozen *n*-octane matrix. This is suggested to be due to several reasons.

(1) Pt(thpy)(CO)(Cl) is planar, and in the crystalline form one finds a columnar arrangement with short Pt−Pt separations of 3.51 Å.[40] At such a short separation one usually finds significant Pt−Pt interactions.[41,42] Therefore, the crystalline material is deeply orange-red colored as compared to the green color of the dissolved material.

(2) From extensive investigations of linear-chain-forming tetracyanoplatinates(II), it is known that the corresponding emission is similarly structured as the low-energy broad-band emission of Figure 1 and that it occurs significantly red shifted relative to the lowest monomer absorption (see below).[41,42]

(3) For the related Pt(ptpy)(CO)(Cl) complex with ptpy = 2-*p*-tolylpyridine, P. Ford et al. have shown that a broad-band and red-shifted emission grows in with increasing concentration. This emission was also assigned to result from oligomers.[14]

The structured part of the emission lying in the green-yellow region of the spectrum (Figure 1) results from a different emitter. This is proven by the fact that, by use of a selective excitation, for example, at 22952 cm^{-1} (435.69 nm), one obtains only the well-structured part of the emission without any broad-band contribution. (Compare Figure 2.) This structured emission is assigned to stem from *monomers* of Pt(thpy)(CO)(Cl). The excitation energy chosen is identified as the electronic origin of the lowest singlet−singlet transition of the monomer sitting in the *n*-octane matrix cage.[35] In the following discussion, the corresponding excited singlet state is designated as S_1 (see also below). It is the focus of this investigation to study mainly triplet emission properties of the monomers.

3.2. Low-Energy Electronic Origins and Decay Times of Monomeric Pt(thpy)(CO)(Cl). A selective excitation at the energy of the $S_0 \rightarrow S_1$ electronic origin at 22952 cm^{-1} of Pt(thpy)(CO)(Cl) leads to the well-structured one-site emission spectrum reproduced in Figure 2. An assignment of the different lines observed requires at first the identification of the three electronic origins (0−0 transitions) corresponding to the triplet substates I, II, and III. This is accomplished by comparing the line structures at the high-energy side of the emission to the structures at the low-energy side of the excitation spectrum. In Figure 3, the spectral region of the electronic origins is reproduced on an enlarged scale. At $T = 1.2$ K, one observes emission peaks at 18012.5

(40) Engebretsen, T.; Kvam, P.-I.; Lindeman, S. V.; Songstad, J. *Acta Chem. Scand.* **1995**, *49*, 853.
(41) Yersin, H.; Gliemann, G. *Ann. N. Y. Acad. Sci.* **1978**, *313*, 539.
(42) Gliemann, G.; Yersin, H. *Struct. Bonding (Berlin)* **1985**, *62*, 87.

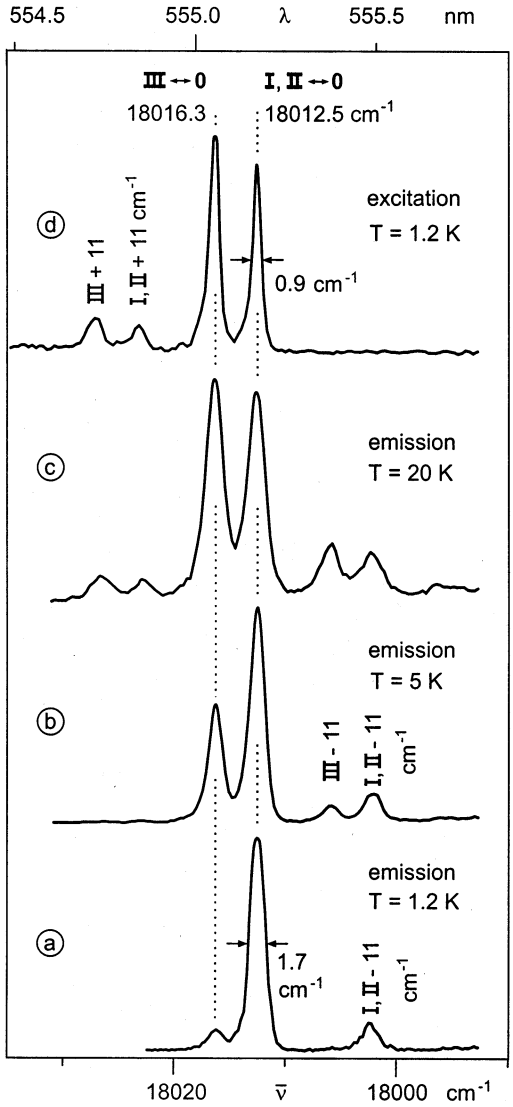

Figure 3. Triplet emission and triplet excitation spectra of Pt(thpy)(CO)(Cl) monomers in *n*-octane in the region of the electronic origins 0 ↔ I/II and 0 ↔ III at different temperatures. The emission spectra (a−c) are selectively excited at 22952 cm^{-1} (435.69 nm, $S_0 \rightarrow S_1$ 0−0 transition). The excitation spectrum (d) is selectively detected at 17298 cm^{-1} (715 cm^{-1} vibrational satellite in emission from the triplet substates I/II; compare Figure 2).

and 18016.3 cm^{-1} (Figure 3a). These are assigned to the transitions I/II ↔ 0 and III ↔ 0, respectively. (The small peak lying 11 cm^{-1} at the low-energy side of the I/II ↔ 0 transition represents a matrix cage or lattice mode satellite; see below.) With a temperature increase, the electronic origin III ↔ 0 at 18016.3 cm^{-1} lying 3.8 cm^{-1} above the origins I/II ↔ 0 gains intensity and also the corresponding 11 cm^{-1} phonon satellite grows in (Figure 3b,c). As expected, the electronic origins are also clearly observable in an excitation spectrum. (See the line-narrowed spectrum shown in Figure 3d.)

The assignments presented are supported additionally: The peak at 18012.5 cm^{-1} consists really of two electronic transitions, I ↔ 0 and II ↔ 0, as proposed above, although the line-narrowed spectrum with a half-width of about 0.9 cm^{-1} (Figure 3d) does not reveal any splitting. Obviously, it is too small to be observable by the technique applied. However, the energy separation between states I and II can directly be determined to be 0.05437 cm^{-1} (1631 MHz) by use of the powerful method of ODMR spectroscopy (section 3.4). Moreover, the observation of two emission decay components at $T = 1.2$ K of $\tau_I = 120$ μs and $\tau_{II} = 45$ μs gives an independent confirmation for two only slightly split triplet substates, I and II.[20,21] This two-component decay behavior is a consequence of a population of the two states I and II by intersystem crossings after an excitation of the higher lying singlet, for example, and of a very slow spin−lattice relaxation between these two triplet substates at low temperature.[18−21,43,44] It can be shown that the SLR time between these states is much longer than $\tau_I = 120$ μs (e.g., compare refs 18−21).

Usually, one does not have direct experimental access to the emission lifetime τ_{III}, which is governed by the decay of the triplet substate III to the electronic ground state 0. However, this decay time can be determined indirectly from the temperature dependence of the long-lived decay component, i.e., after thermal equilibration among all three substates is attained. (Compare also refs 45 and 46.) This procedure has been carried out similarly as described in ref 20 (eq 26), and we obtained $\tau_{III} = 35 \pm 5$ μs.[47]

The intensity ratio of the two origin lines at 18016.3 cm^{-1} (III → 0) and 18012.5 cm^{-1} (I/II → 0) does not seem to be consistent with the assignment given. In particular, when a fast thermal equilibration is assumed to govern the emission intensity ratio of the transitions III → 0 and I/II → 0, one would expect that the higher lying peak at 18016.3 cm^{-1} (III → 0) should be about 1 order of magnitude less intense than is observed at $T = 1.2$ K (Figure 3a). However, slow spin−lattice relaxation also determines this intensity ratio. Generally, at small energy separations (e.g., several cm^{-1}) between different electronic states, a Boltzmann distribution is not attained at low temperature.[18,21] Thus, it is well consistent that the emission of state III cannot be frozen out. Moreover, at low temperature, state III emits with a specific emission decay time that is mainly given by the relaxation times from state III to states I and II (and not by the decay time τ_{III}). The corresponding SLR time has been determined to be as long as τ_{SLR}(III ⇝ I, II) = 3 μs.[18−21] Correspondingly, the same value is found as an emission *rise* when state III is selectively excited and when the emissions of the triplet substates I and II are selectively detected.[18−21]

For completeness, it is mentioned that we could not detect any fluorescence of the lowest excited singlet S_1 lying at 22952 cm^{-1}. Its singlet character is proven by the observation that the corresponding state does not exhibit any Zeeman splitting or shift.[35] (Selective excitation of this state was used to obtain the well-structured triplet emission spectrum shown in Figure 2.) Nevertheless, we could estimate the lifetime of the singlet state to $\tau(S_1) \approx 5$ ps.[35] This value is deduced

(43) Scott, P. L.; Jeffries, C. D. *Phys. Rev.* **1992**, *127*, 32.
(44) Abragam, A.; Bleany, B. *Electron Paramagnetic Resonance of Transition Ions*; Clarendon Press: Oxford, U.K., 1989.
(45) Azumi, T.; O'Donell, C. M.; McGlynn, S. P. *J. Chem. Phys.* **1966**, *45*, 2735.
(46) Harrigan, R. W.; Crosby, G. A. *J. Chem. Phys.* **1973**, *59*, 3468.
(47) Strasser, J. Ph.D. Thesis, Universität Regensburg, Germany, 1999.

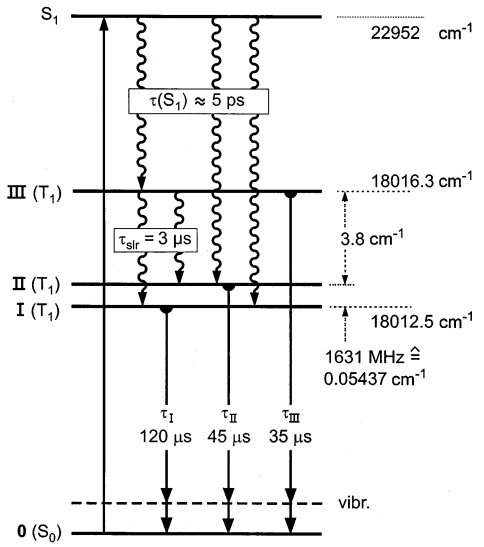

Figure 4. Energy level scheme and decay times for Pt(thpy)(CO)(Cl) monomers in *n*-octane at $T = 1.2$ K. The sequence of the triplet substates I and II is not known. The decay time of S_1 is estimated from the homogeneous line width of the $S_0 \rightarrow S_1$ 0−0 transition.[35] The value of the decay time τ_{III} (35 μs) is determined indirectly in ref 47 from the temperature dependence of the long-lived decay component.

from an estimate of the homogeneous half-width of about 1 cm^{-1} of the $S_0 \rightarrow S_1$ 0−0 transition (Lorentzian line shape; compare ref 18, eq 2, and refs 27 and 48). Such an assignment is based on the condition that pure dephasing is slow. This, however, is very likely under the experimental conditions applied (low temperature, low chromophore concentration) due to relatively weak electron−phonon coupling and the weak interaction between the chromophores. Presumably, the decay time $\tau(S_1)$ is largely controlled by the depopulation of S_1 due to intersystem crossing from S_1 to T_1. The value estimated for Pt(thpy)(CO)(Cl) is remarkably long as compared to the decay time of S_1 of $Pt(thpy)_2$, which has been determined similarly to be about 50 fs.[18] The 2 orders of magnitude shorter time constant found for the latter compound seems to be related mainly to the significantly larger effective spin−orbit coupling in $Pt(thpy)_2$.[18] We remark that the nomenclature used to designate the lowest excited singlet state as S_1 does not imply any assignment to specific orbital characters. A corresponding classification is not yet possible. Detailed ab initio calculations can result in such an assignment, as has been carried out, for example, for $Pt(thpy)_2$.[49]

The results concerning the electronic origins and the decay times discussed are summarized in an energy level diagram shown in Figure 4.

3.3. Vibrational Satellite Structure. The line structure of Figure 2 observed at the low-energy side of the electronic 0−0 transitions at 18012.5 cm^{-1} (I/II → 0) is assigned to satellites which are induced by lattice or cage vibrations of the matrix (including librations) (e.g., 11 and 96 cm^{-1}) and by complex vibrations. In the energy range below about 600 cm^{-1}, the vibrations may contain significant metal−ligand (M−L) vibrational character (e.g., 445 and 508 cm^{-1}), while those modes of higher energy (e.g., 715, 1400, and 1490 cm^{-1}) represent internal thpy ligand vibrations. (Compare, e.g., ref 18, p 92, and ref 50.) One also observes combinations of complex vibrations with lattice modes (e.g., 381 + 11 and 715 + 11 cm^{-1}) and combinations of different complex vibrations (e.g., 715 + 381, 715 + 635, and 1490 + 381 cm^{-1}). Also two Franck−Condon progressions (1 × 11 and 2 × 11 cm^{-1} and 1 × 715 and 2 × 715 cm^{-1}) are seen. According to the small value of the maximum Huang−Rhys parameter (compare refs 18 and 51) of $S_{max} = 0.2 \pm 0.05$ found for these two progressions, one can conclude very small shifts of the equilibrium positions of the emitting triplet substates I and II relative to the electronic ground state 0.

A careful inspection of the satellite structure reveals that almost all satellites have weak shoulders occurring at about 4 cm^{-1} on the high-energy sides. These peaks are attributed to the overlapping emission of state III, which lies 3.8 cm^{-1} above states I and II (see Figure 4).

The high intensity found at the electronic origin of the 0−0 transitions I/II → 0 relative to the intensities of the vibrational satellites reflects the information that *direct* spin−orbit coupling to the triplet substates I/II is effective and that this mechanism provides intensities to the 0−0 transitions and to those vibrational satellites that are induced by Franck−Condon activity. These satellites borrow their intensities from the intensities of the purely electronic transitions I/II → 0. The Franck−Condon activity is directly proven for those cases for which progressions are observed (11 and 715 cm^{-1} modes). Presumably, the other vibrational satellites are also Franck−Condon induced, though with smaller Huang−Rhys parameters. This assignment for the intensity mechanism of the vibrational satellites is proposed, because alternative intensity providing mechanisms according to vibronic coupling to higher lying states are usually of minor importance when *direct* spin−orbit coupling is significant and when the intensity at the electronic origin strongly dominates. (For background information compare refs 18 (p 129 ff), 23, and 51−54.)

Interestingly, most of the more intense satellites occurring in the emissions of states I and II (Figure 2) correspond to vibrational satellites of $Pt(thpy)_2$,[18,23] which are also significantly intense. For example, the internal ligand vibrations at 1036, 1118, 1400, and 1490 cm^{-1} of Pt(thpy)(CO)(Cl) can be correlated to the vibrations at 1030, 1123, 1400, and 1484 cm^{-1} of $Pt(thpy)_2$, while in the energy range of the M−L vibrations a correlation is difficult, if a normal coordinate analysis is not available. Presumably, the good correspondence in energy of the 381 cm^{-1} mode of Pt(thpy)-

(48) Demtröder, W. *Laser-Spektroskopie*; Springer: Berlin, 1991; p 42 ff.
(49) Pierloot, K.; Ceulemans, A.; Merchán, M.; Serrano-Andrés, L. *J. Phys. Chem. A* **2000**, *104*, 4374.
(50) Flint, C. D.; Matthews, A. D. *J. Chem. Soc., Faraday Trans. 2* **1976**, *72*, 579.
(51) Brunold, T. C.; Güdel, H. U. In *Inorganic Electronic Structure and Spectroscopy*; Solomon, E. I., Lever, A. B. P., Eds.; Wiley: New York, 1999; Vol. 1, p 259.
(52) Hochstrasser, R. M. *Molecular Aspects of Symmetry*; W. A. Benjamin Inc.: New York, Amsterdam, 1966.
(53) Flint, C. D., Ed. *Vibronic Processes in Inorganic Chemistry*; NATO ASI Series C; Kluwer Academic Publishers: Dordrecht, The Netherlands, 1989; Vol. 288.
(54) Yersin, H.; Humbs, W.; Strasser, J. *Top. Curr. Chem.* **1997**, *191*, 153.

(CO)(Cl) to the 383 cm^{-1} mode of $Pt(thpy)_2$ may be taken as an indication that this mode is also dominated by internal ligand vibrational character.

Moreover, in ref 18 (p 140), it has been proposed that the two vibrational modes of $Pt(thpy)_2$ of 713 and 718 cm^{-1} are the nontotally and totally symmetric combinations, respectively, of single-ligand modes. In this case, the energy splitting of 5 cm^{-1} would correspond to the energy of the vibrational ligand−ligand coupling for this specific mode. The observation of just one single vibrational mode of 715 cm^{-1} for Pt(thpy)(CO)(Cl), having an energy approximately in the middle between these plus and minus combinations of the vibrational modes of $Pt(thpy)_2$, supports the interpretation given previously.[18]

For completeness, it is mentioned that a very weak vibrational satellite of 1918 cm^{-1} occurs in the emission spectra of the triplet substates I/II (not reproduced in Figure 2).[35] Since this satellite does not fit any combination of the other vibrational modes observed, it is assigned to correspond to a fundamental mode. It is suggested that this mode is the C−O stretching vibration. Usually, C−O vibrations occur at slightly higher energies in neutral transition-metal complexes.[55] For example, in ref 56 a value of 2053 cm^{-1} is reported for $Pt(CO)_4$. Thus, it is indicated that in Pt(thpy)-(CO)(Cl) the force constant of the C−O vibration is slightly smaller than in other compounds. Indeed, this fits the observation that the C−O bond length in Pt(thpy)(CO)(Cl) of 1.166 Å[40] is slightly larger than normally found (typical value 1.145 Å[57]). Interestingly, the occurrence of a C−O satellite in the emission spectrum reflects a change of the electronic charge distribution with an electronic $T_1 \leftrightarrow S_0$ transition also in the spatial region of the CO ligand. (Compare refs 18 (p 160), 22, 54 (p 199), and 58.)

3.4. Optically Detected Magnetic Resonance. In section 3.2, it is shown that all three triplet substates of Pt(thpy)-(CO)(Cl) are emissive. The ZFS or the triplet-state fine structure splitting between the two lower lying substates I/II and the third state III was determined to be 3.8 cm^{-1} (Figure 4). On the other hand, the second zero-field splitting parameter characteristic of a triplet state could not be resolved. However, it is very probable that this latter ZFS parameter lies in the microwave range available with our ODMR equipment. Therefore, we have conducted optically detected magnetic resonance experiments at zero and low magnetic fields. Indeed, applying microwave excitation in the frequency range from 0.1 to 8 GHz, just *one* zero-magnetic-field ODMR signal is observed (at 1.4 K). The ODMR transition, detected at the electronic origin at 18012.5 cm^{-1} (555.17 nm) of the emission spectrum, is reproduced in Figure 5. The microwave frequency corresponding to the maximum of the zero-field resonance is 1631 MHz (0.05437 cm^{-1}). The characteristic line width (fwhm) of the zero-field transition is 40 MHz.

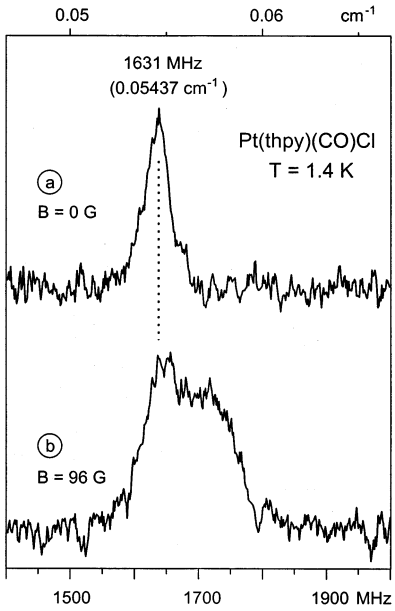

Figure 5. (a) Zero-field ODMR transition for Pt(thpy)(CO)(Cl) monomers in an *n*-octane Shpol'skii matrix in the photoexcited triplet state. Photoexcitation at 340 nm (~29400 cm^{-1}), detection at 555.17 nm (18012.5 cm^{-1}), $T = 1.4$ K, $c \approx 10^{-5}$ mol/L. (b) Same conditions as in (a) but in the presence of an externally applied magnetic field of 96 G.

Table 1. Microwave Frequencies for the Maxima of ODMR Transitions and Line Widths of Photoexcited Pt(thpy)(CO)(Cl) in *n*-Octane for Various Magnetic Fields ($T = 1.4$ K)

B (G)	0	100	200	290
resonance frequency (MHz)	1631	1658	1720	~1750
fwhm (MHz)	40	125	320	350

This ODMR transition appeared sensitive to the application of small magnetic fields (<400 G). As the magnetic field is increased, the ODMR signal slightly shifts to higher frequencies (positive frequency shift) and shows an asymmetric broadening with its steepest slope on the low-frequency side and the total integrated intensity rapidly decreases. When fields higher than about 400 G are applied, the ODMR signal becomes too weak to be reliably studied. In Table 1 the main features of the ODMR transitions are collected for a few magnetic field strengths.

As discussed by McCauley et al.[59,60] for a triplet state with $D \geq 3E > 0$ in the low-field limit, the ODMR transition as detected for an ensemble of randomly oriented molecules in the triplet state is expected to exhibit positive resonance frequency shifts for the $2E$ and $D + E$ zero-field transitions and a negative shift for the $D - E$ transition upon application of a weak magnetic field. Also, the $2E$ transition will be asymmetrically broadened with the steepest slope on the low-frequency wing.[59−61] All these features are observed for the

(55) Nakamoto, K. *Infrared and Raman Spectra of Inorganic and Coordination Compounds*; John Wiley: New York, 1978.
(56) Kündig, E. P.; McIntosh, D.; Moskovits, M.; Ozin G. A. *J. Am. Chem. Soc.* **1973**, *95*, 7234.
(57) Wilson, A. J. C., Prince, E., Eds. *International Tables for Crystallography*; Kluwer Academic Publishers: Dordrecht, The Netherlands, 1999; Vol. C, p 813.
(58) Gastilovich, E. A. *Sov. Phys. Usp. (Engl. Transl.)* **1991**, *34*, 592.
(59) McCauley, E. M.; Lasko, C. L.; Tinti, D. S. *Chem. Phys. Lett*. **1991**, *178*, 109.
(60) McCauley, E. M.; Lasko, C. L.; Tinti, D. S. *J. Phys. Chem.* **1992**, *96*, 1146.
(61) The parameters D and E are the fine structure parameters that are usually used to describe the zero-field splittings of triplet states of organic molecules due to spin−spin interactions (for example, compare refs 25, 31, and 62).

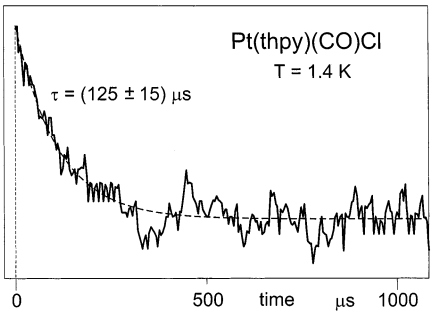

Figure 6. Zero-field optically detected microwave recovery transient for photoexcited Pt(thpy)(CO)(Cl) monomers in an *n*-octane Shpol'skii matrix at $T = 1.4$ K and $c \approx 10^{-5}$ mol/L (intensity on a linear scale). The microwave pulse applied is at 1631 MHz corresponding to the splitting of the two lower triplet substates I and II ($2E$ splitting); $t = 0$ corresponds to the time when the microwave pulse is switched "off". The drawn curve is the best fit to a monoexponential decay of $\tau = 125 \pm 15$ μs. This value corresponds to the emission decay constant of triplet substate I of $\tau_I = 120$ μs as determined by emission decay experiments (see section 3.2).

ODMR transition studied (Figure 5). Considering that one of the fine structure splitting parameters is 3.8 cm^{-1} (Figure 4), it is concluded that the zero-field resonance at 1631 MHz corresponds to the hitherto unobserved $2E$ zero-field transition between substates I and II.

Applying at zero magnetic field a microwave pulse of 1631 MHz being in resonance with the energy splitting of triplet substates I and II, while cw optical excitation is maintained, one obtains the ODMR microwave recovery transient presented in Figure 6. This transient shows an "instantaneous" rise following the microwave pulse, whereas the decay part is representative of the population recovery during the time that the microwave intensity is turned off. The recovery is fitted to an exponential decay function for which the best fit value of the decay time is 125 ± 15 μs at 1.4 K. On the other hand, the emission decay times for the two states I and II (at 18012.5 cm^{-1}) have been determined to be 120 and 45 μs[19−21] (section 3.2 and Figure 4). Thus, it may be concluded that the longer component is reproduced in the microwave recovery experiment. The instantaneous rise needs some further comment. The microwave recovery experiment was performed while cw optical pumping of the triplet state was maintained. Consequently, the rise component is also determined by the optical feeding rate. In addition, the time resolution in the experiment is limited by the applied load resistance for the photomultiplier (100 kΩ). This limits the resolution to about 30 μs. (The error of ±15 ms in the fitted decay is the estimated error in the fitting of the time constant.) For these reasons fitting to a biexponential function with a short component of about 40 μs (the lifetime of substate II) or less is not meaningful.

In summary, it is worth noting that the lowest triplet state of Pt(thpy)(CO)(Cl) is an example for which the determination of its fine structure splittings has become possible by the application of powerful complementary techniques: high-resolution optical spectroscopy and optical-microwave double resonance. In addition, it has been possible by these two techniques to independently determine triplet substate lifetimes. For Pt(II) compounds, this procedure is carried out for the first time.

4. Assignments, Comparisons, and Trends

The lowest triplet state of Pt(thpy)(CO)(Cl) has been characterized by complementary methods, such as high-resolution optical investigations and ODMR measurements at low temperatures. Thus, the zero-field splittings of the three triplet substates of T_1 I, II, and III, could be determined. In particular, the splitting between states I and II is $\Delta E_{I,II} = 0.05437$ cm^{-1} (1631 MHz), while the energy separation from these two states, I/II, to substate III is with $\Delta E_{I,III} = 3.8$ cm^{-1} a factor of 70 larger (Figure 4).

Whereas the small ZFS between substates I and II could in principle contain contributions arising from spin−spin couplings (usually on the order of 0.1 cm^{-1}; compare refs 31 and 62), a ZFS of 3.8 cm^{-1} is clearly a consequence of spin−orbit coupling according to Pt 5d and/or MLCT character in the low-lying triplet state.[18,25,54] The importance of spin−orbit coupling for Pt(thpy)(CO)(Cl) is also evidenced by the observation of relatively intense excitation peaks at the electronic origins corresponding to absorptions from the singlet ground state to the triplet substates (Figure 3d).

On the other hand, the size of the total ZFS of 3.8 cm^{-1} is still small when compared to the values found for typical ^{3}MLCT states of compounds such as $[Ru(bpy)_3]^{2+}$ and $[Os(bpy)_3]^{2+}$, for which the values of ZFSs are as large as 61 and 211 cm^{-1}, respectively.[18,54] This comparison shows that the Pt 5d/MLCT character in Pt(thpy)(CO)(Cl) is still relatively small. Several other results support this message.

(i) The intensities of vibrational satellites of metal−ligand character (below ∼600 cm^{-1}), being representative of metal contributions, are relatively small for Pt(thpy)(CO)(Cl) as compared to those of compounds with significant MLCT character in the lowest triplets as found for $Pt(thpy)_2$, $[Ru(bpy)_3]^{2+}$, and $[Os(bpy)_3]^{2+}$.[18,23,54,58,63]

(ii) The maximum Huang−Rhys parameter, which characterizes the extent of geometry change between electronic ground and excited states, becomes *smaller* with increasing MLCT contribution. For example, compounds with significant MLCT character exhibit values for the $S_0 \rightarrow T_1$ transitions of $S_{max} \leq 0.1$, while for Pt(thpy)(CO)(Cl) an at least 100% larger value of $S_{max} = 0.2$ is found. (Compare refs 18 (p 170), 23, 54 (p 237), and 63.)

(iii) Finally, the energy separation between the lowest singlet state S_1 and the triplet state T_1, $\Delta E(S_1-T_1)$, approximately representing twice the exchange interaction, follows the same trend and reflects the smaller metal participation in the T_1 state of Pt(thpy)(CO)(Cl). For this compound one finds $\Delta E(S_1-T_1) = 4936$ cm^{-1}, while $Pt(thpy)_2$ with a significant MLCT contribution exhibits a much smaller singlet−triplet splitting of $\Delta E(S_1-T_1) = 3278$ cm^{-1} (ref 18, p 171). This smaller value of the latter compound reflects the larger delocalization of the excitation, i.e., the larger spatial extensions of the corresponding wave functions

(62) Clarke, R. H., Ed. *Triplet State ODMR Spectroscopy*; Wiley: New York, 1982.
(63) Yersin, H.; Huber, P.; Wiedenhofer, H. *Coord. Chem. Rev.* **1994**, *132*, 35.

Table 2. ZFSs and Transition Energies of Monochelated and Bischelated Organometallic Pt(II) Compounds

compound[a]	transition energy of $\mathbf{I} \rightarrow \mathbf{0}$[b] ($cm^{-1}$)	zero-field splitting $\Delta E_{I,II}$[c] (cm^{-1})	zero-field splitting $\Delta E_{I,III}$[c] (cm^{-1})	assignment	ref
Pt(i-biq)$(CN)_2$[d,e]	~19000	0.00367 (110 MHz)	0.157 (4765 MHz)		13
Pt(thpy)(CO)(Cl)[f]	18012.5	0.05437 (1631 MHz)	3.8		this work
Pt(ppy)(CO)(Cl)[f,g]	20916	<0.5	6.4	^{3}LC($^3\pi\pi^*$) + increasing MLCT admixtures	18, 19, 35
Pt(dppy)(CO)[d,f,h]	19174.5	<0.5	17.5		65
Pt$(thpy)_2$[f]	17156	7	16		18, 22, 23
Pt$(ppy)_2$[f]	19571	6.9	32		18, 20, 66

[a] Compare Figure 7. [b] Lowest triplet substate I and singlet ground state 0. [c] $\Delta E_{I,II}$ = ZFS between the two lowest triplet substates I and II (2*E* splitting); $\Delta E_{I,III}$ = total ZFS ($|D| + E$ splitting) (compare Figure 4). [d] Compound given for comparison. [e] i-biq = 2,2′-bisisoquinoline (bidentate ligand); Pt(i-biq)$(CN)_2$ dissolved in dimethylformamide (ref 13). [f] Compound dissolved in *n*-octane (Shpol'skii matrix). [g] $(ppy)^-$ = phenylpyridinate (bidentate ligand). [h] $(dppy)^-$ = diphenylpyridinate (tridentate ligand).

into the region of the metal (and the second (thpy) ligand[22]). (Compare also ref 64, p 31.)

In conclusion, the lowest excited triplet T_1 of Pt(thpy)(CO)(Cl) can be assigned as a ligand-centered (LC) state of $^3\pi\pi^*$ character with small MLCT admixtures. The electronic wave functions of the T_1 state slightly extend also to the CO ligand.

Interestingly, not only does the *size* of the total zero-field splitting of the triplet reflect characteristic properties, but also the *splitting patterns* point to specific trends. Table 2 compares the values of ZFSs of Pt(thpy)(CO)(Cl) to those of three other Pt(II) complexes with coordination of only *one* organic ligand consisting of aromatic rings. (Compare Figure 7.) In all four cases, the splittings between the two lower lying triplet substates I and II are significantly smaller than the energy separations from these two states to triplet substate III. However, with coordination to a second aromatic chelate, which leads to homoleptic compounds such as Pt$(thpy)_2$ or Pt$(ppy)_2$, the splitting patterns change drastically. This is particularly clear when the ZFSs of Pt(thpy)(CO)(Cl) are compared to those of Pt$(thpy)_2$. The ratio $\Delta E_{I,III}/\Delta E_{I,II}$ decreases from 70 to 2.3.

Moreover, the total ZFS increases by a factor of 4.2 and 5, when heteroleptic Pt(thpy)(CO)(Cl) and Pt(ppy)(CO)(Cl), respectively, are compared to the corresponding homoleptic compounds (Table 2). This allows us to conclude a strong increase of MLCT participation in the lowest triplet state by chelation of two ligands. It is proposed that this interesting property can be traced back to relative shifts of the ligand π, ligand π^*, and Pt 5d orbitals. It seems further that the electronic coupling between the two ligands in the homoleptic compounds plays a crucial role. For Pt$(thpy)_2$, for example, it has been shown recently[18,22] that the T_1 state is delocalized over the metal and the two ligands. This implies

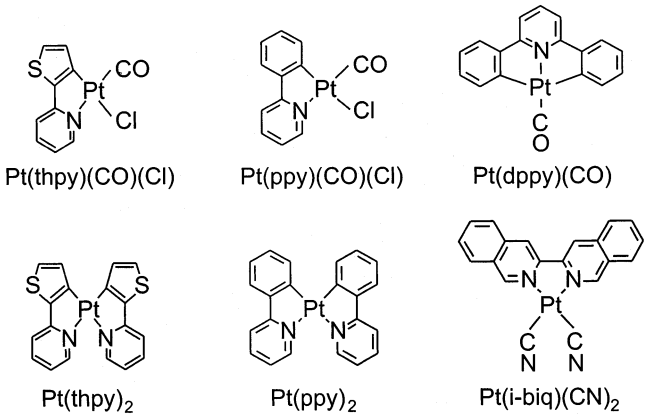

Figure 7. Chemical structures of organometallic Pt(II) chelates with different zero-field splittings and thus different MLCT participations in the lowest excited states (see Table 2). The cyclometalated compounds shown are frequently also slightly differently abbreviated; i.e., Pt(thpy)(CO)(Cl) = Pt(2-thpy)(CO)(Cl), Pt(ppy)(CO)(Cl) = Pt(phpy)(CO)(Cl), Pt(dppy)(CO) = Pt(dphpy)(CO), Pt$(thpy)_2$ = Pt$(2\text{-thpy})_2$, and Pt$(ppy)_2$ = Pt$(phpy)_2$ (compare ref 18).

a C_{2v} point group symmetry[18,22] for Pt$(thpy)_2$. Consequently, the ligands are symmetry-related and exhibit a metal-induced electronic coupling. Obviously, this situation does not apply to Pt(thpy)(CO)(Cl).

In conclusion, singlet−triplet substate coupling routes and strengths are strongly altered when heteroleptic compounds are compared to homoleptic compounds. These latter ones exhibit significantly larger metal participations in the lowest excited triplet states. Obviously, a more detailed description of these effects requires further investigations. In particular, quantum mechanical calculations including spin−orbit coupling, which seem to become possible soon, would be highly desirable.

Acknowledgment. Financial support from the Stiftung Volkswagenwerk is gratefully acknowledged. We also thank Dr. M. Koulikova and Prof. Dr. K. P. Balashev (Russian State Pedagogical University, St. Petersburg) for the preparation of Pt(thpy)(CO)(Cl) and Prof. Dr. P. Ford (University of California, Santa Barbara) and his group for sending us Pt(ppy)(CO)(Cl).

IC020132O

(64) Turro, N. J. *Modern Molecular Photochemistry*; The Benjamin/Cummings Publishing Co.: Menlo Park, CA, 1978.
(65) Kratzer, C.; Koulikova, M. V.; Yersin, H. *Book of Abstracts*, 14th International Symposium on the Photochemistry and Photophysics of Coordination Compounds, Veszprém University Press: Veszprém, Hungary; 2001; p 83.
(66) Wiedenhofer, H. Ph.D. Thesis, Universität Regensburg, Germany, 1994.